

Optimized design of flux chambers for measurement of ammonia emission after field application of slurry with full-scale farm machinery

Supporting material

Johanna Pedersen^{*1}, Sasha D. Hafner¹, Andreas Pacholski², Valthor I. Karlsson³, Li Rong³, Rodrigo Labouriau⁴, Jesper N. Kamp¹

¹ Aarhus University, Department of Biological and Chemical Engineering, Denmark

²Thünen-Institute for Climate-Smart Agriculture, Braunschweig, Germany

³Aarhus University, Department of Civil and Architectural Engineering, Denmark

⁴Aarhus University, Department of Mathematics, Denmark

*Corresponding author. Aarhus University, Blichers Alle 20, DK-8830 Tjele, Denmark.

E-mail addresses: jp@bce.au.dk (J. Pedersen), sasha.hafner@bce.au.dk (S. D. Hafner), vik@efla.is (V. I. Karlsson), andreas.pacholski@thuenen.de (A. Pacholski), li.rong@cae.au.dk (L. Rong), rodrigo.labouriau@math.au.dk (R. Labouriau), jk@bce.au.dk (J. N. Kamp)

Dynamic flux chamber design

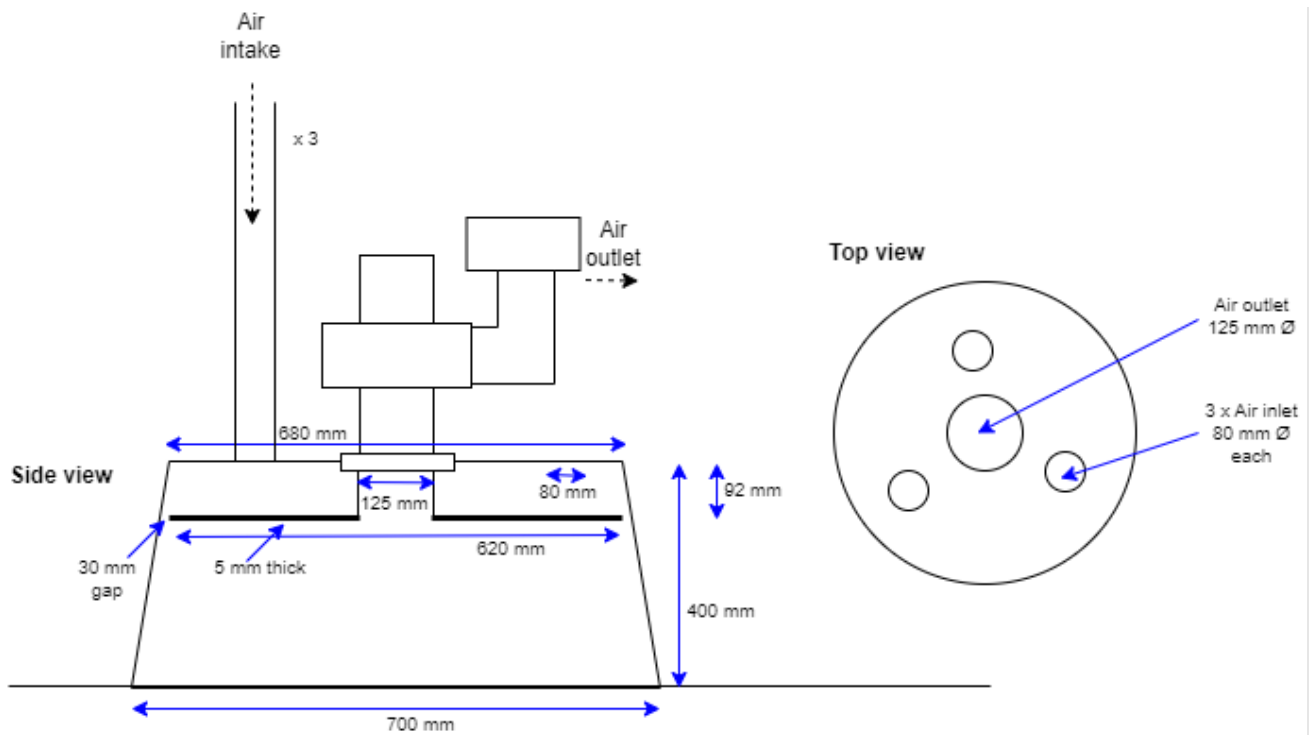


Figure S1. Simplified sketch of dynamic flux chamber with measurements, not to scale.

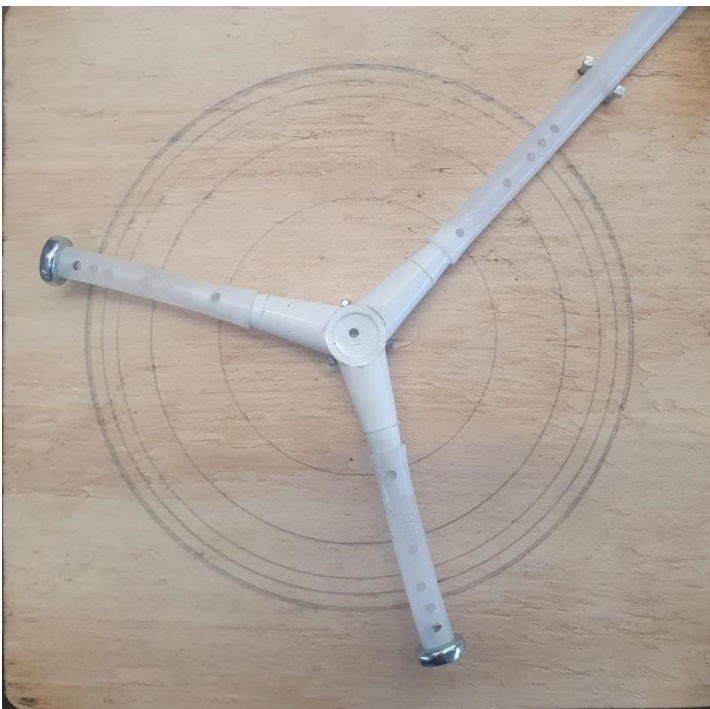


Figure S2. Y-shaped inlet corresponding to the C3u configuration from Table 1 in Loubet et al. (1999).

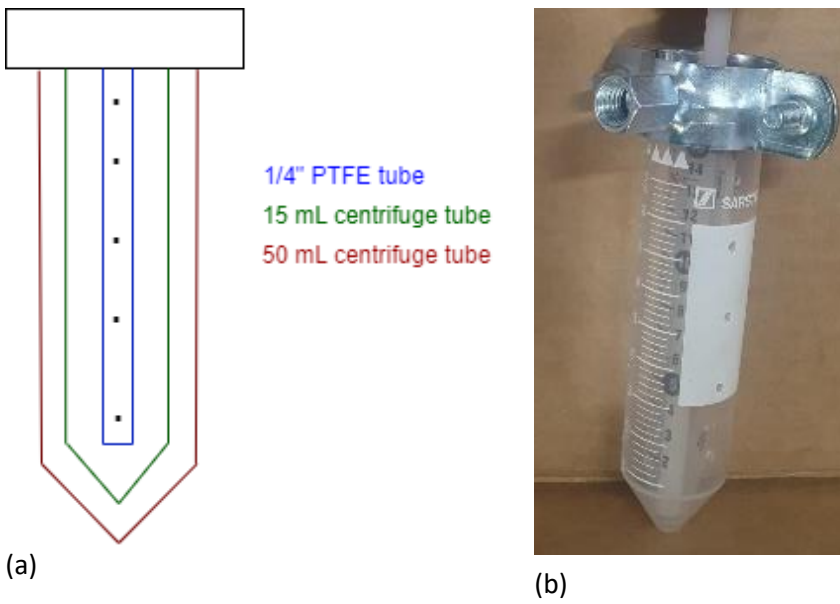


Figure S3. (a) Sketch of air inlet, not to scale. (b) Picture of air inlet.



Figure S4. Dynamic flux chamber in the field with sand sealing at the soil surface.

Field trials

Trial A

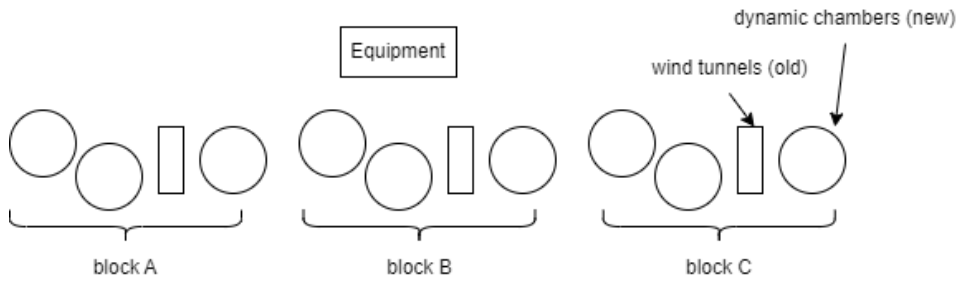


Figure S5. Sketch of overview of trial A, not to scale.



Figure S6. Picture of field layout of trial A.

Trial B

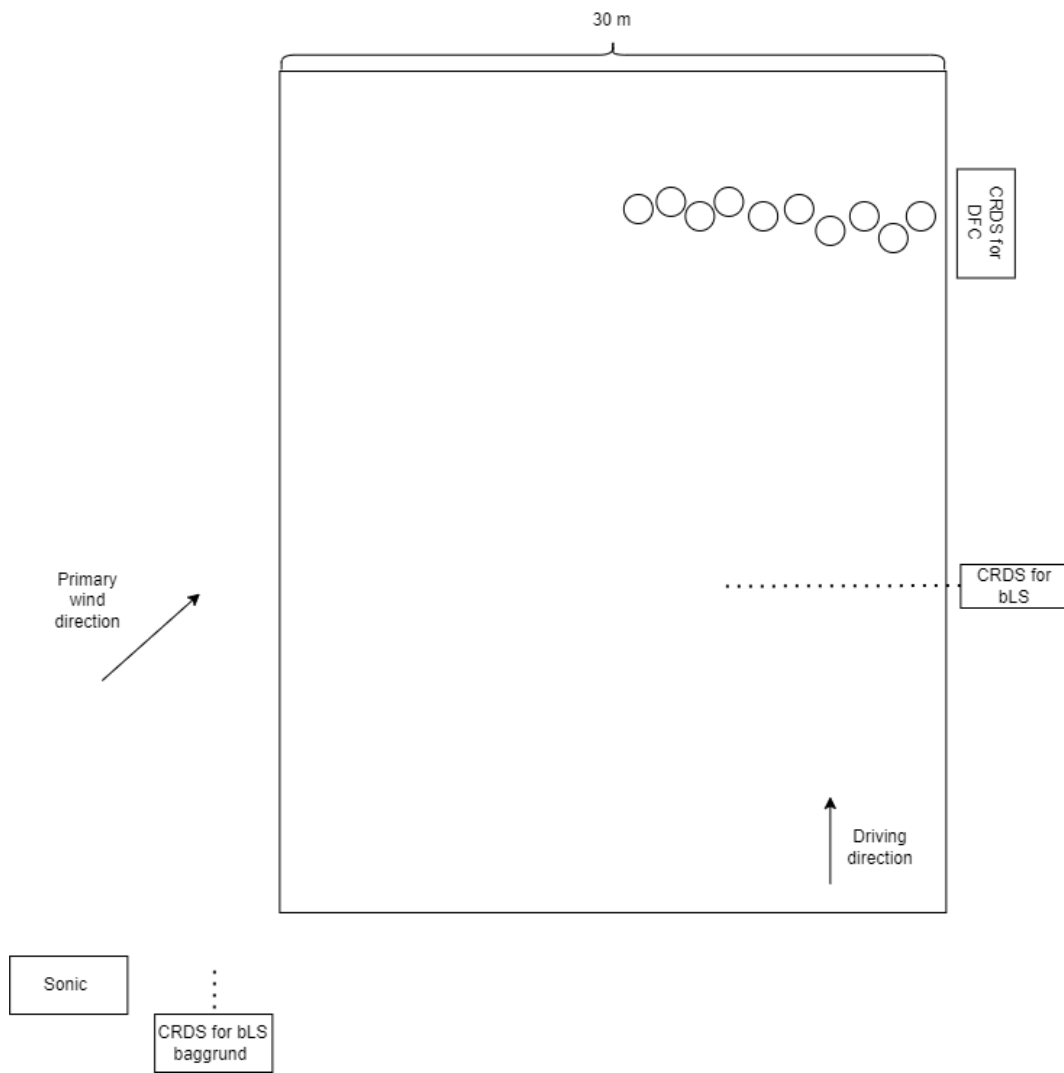


Figure S7. Sketch of field layout for trial B, not to scale.

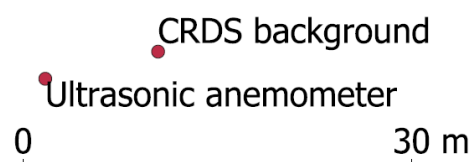
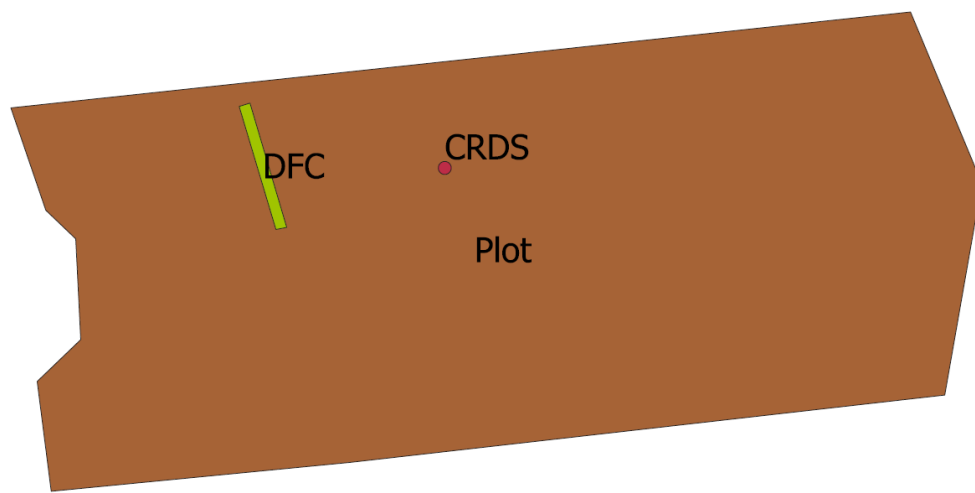


Figure S8. Field layout for trial B mapped with GPS.



Figure S9. Picture of field layout of trial B.

Trial C

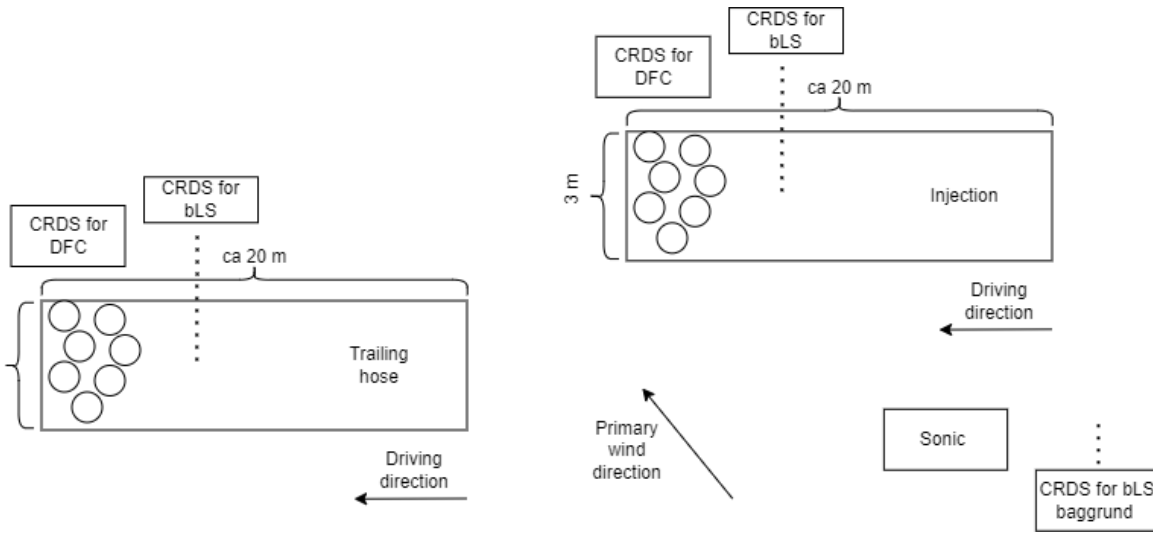


Figure S10. Sketch of field layout for trial C, not to scale.

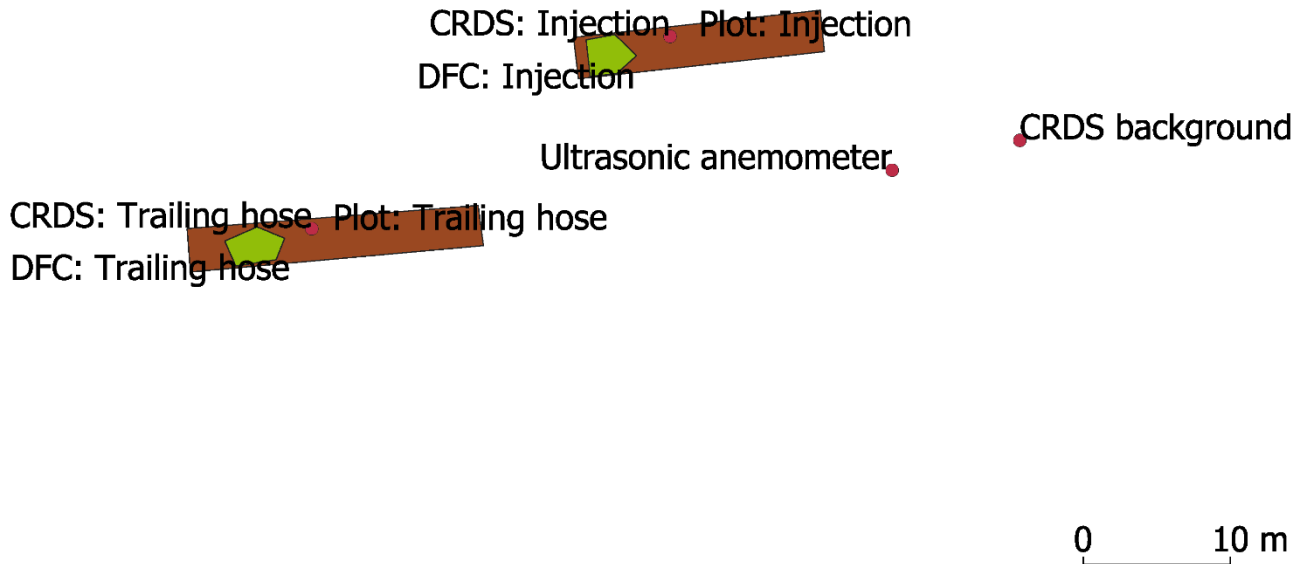


Figure S11. Field layout for trial C mapped with GPS.



Figure S12. Picture of field layout of trial C.



Figure S13. Picture of field layout of trial C.

AER trial

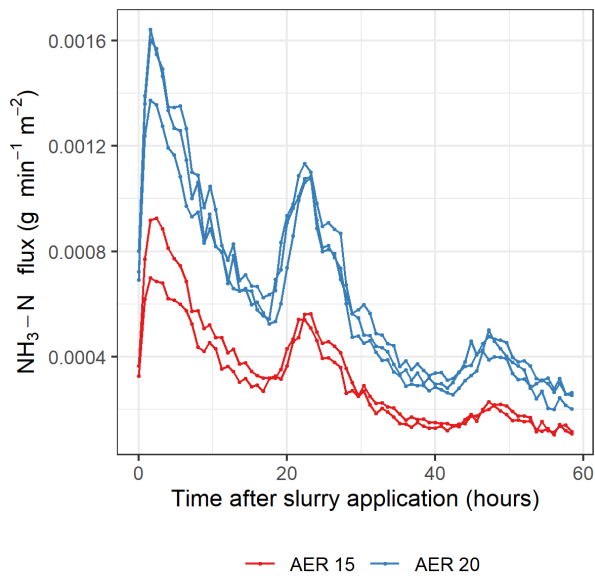


Figure S14. Ammonia flux measured with dynamic flux chambers with two different air exchange rates (AER) after application of cattle slurry.

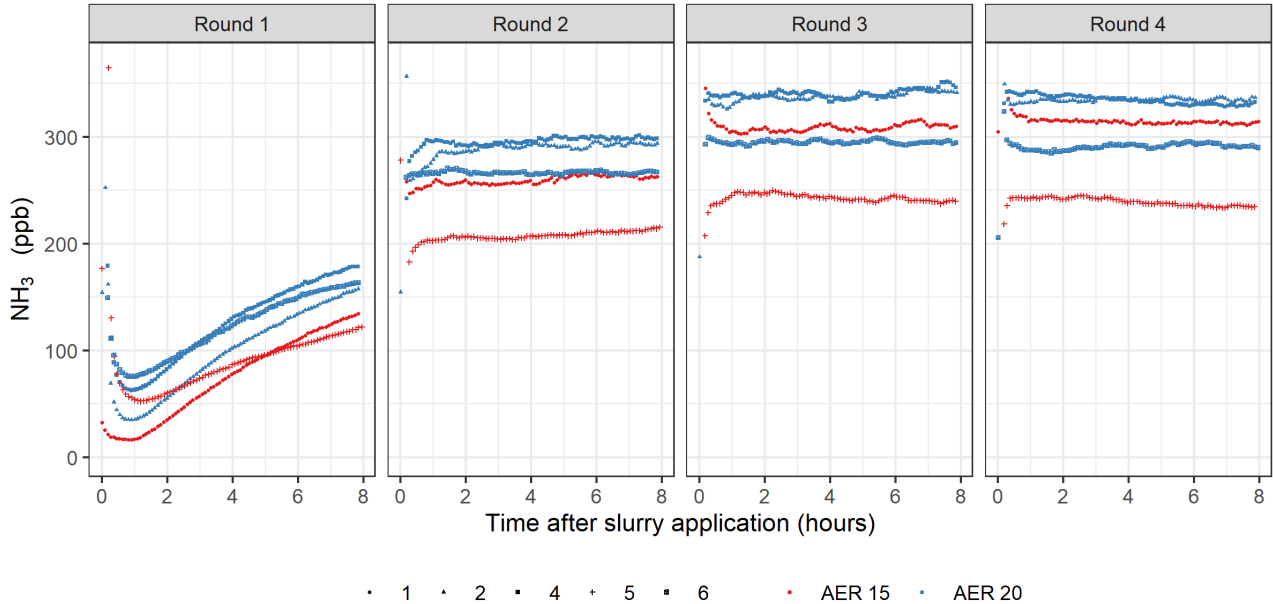


Figure S15. Ammonia concentration measured with dynamic flux chambers with two different air exchange rates (AER) after application of cattle slurry. Measuring round 1-4. Numbers in legend refer to different dynamic chambers.

Statistics

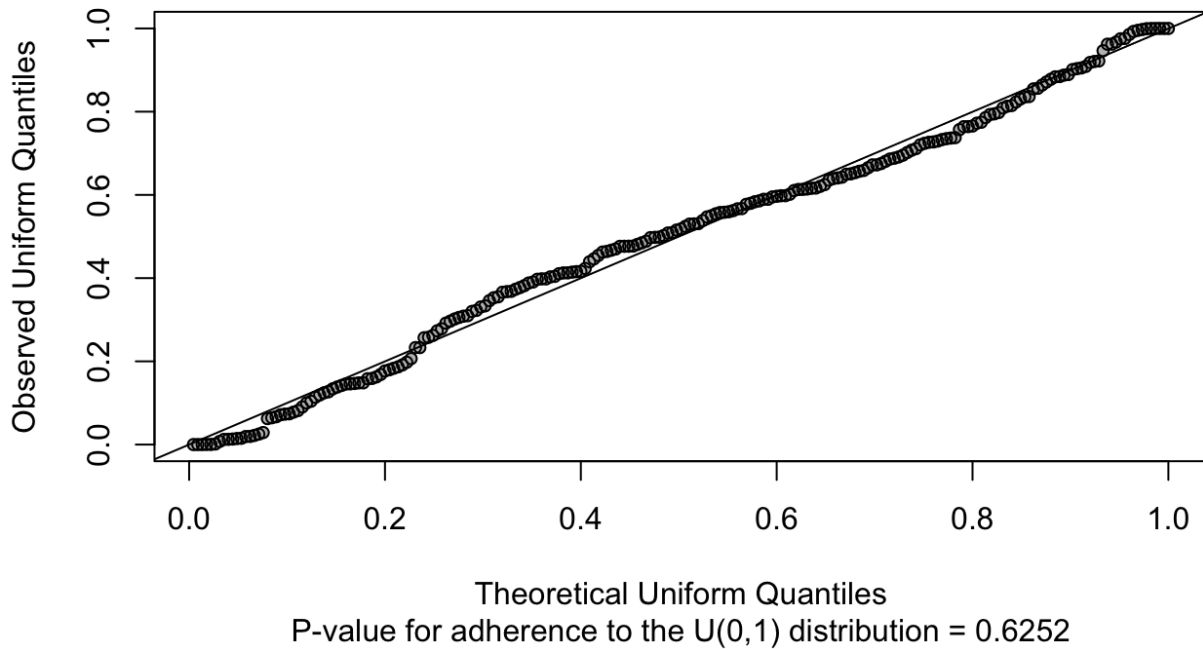


Figure S16. Model control of the Gamma generalized linear mixed model for dynamic flux chambers (DFC).

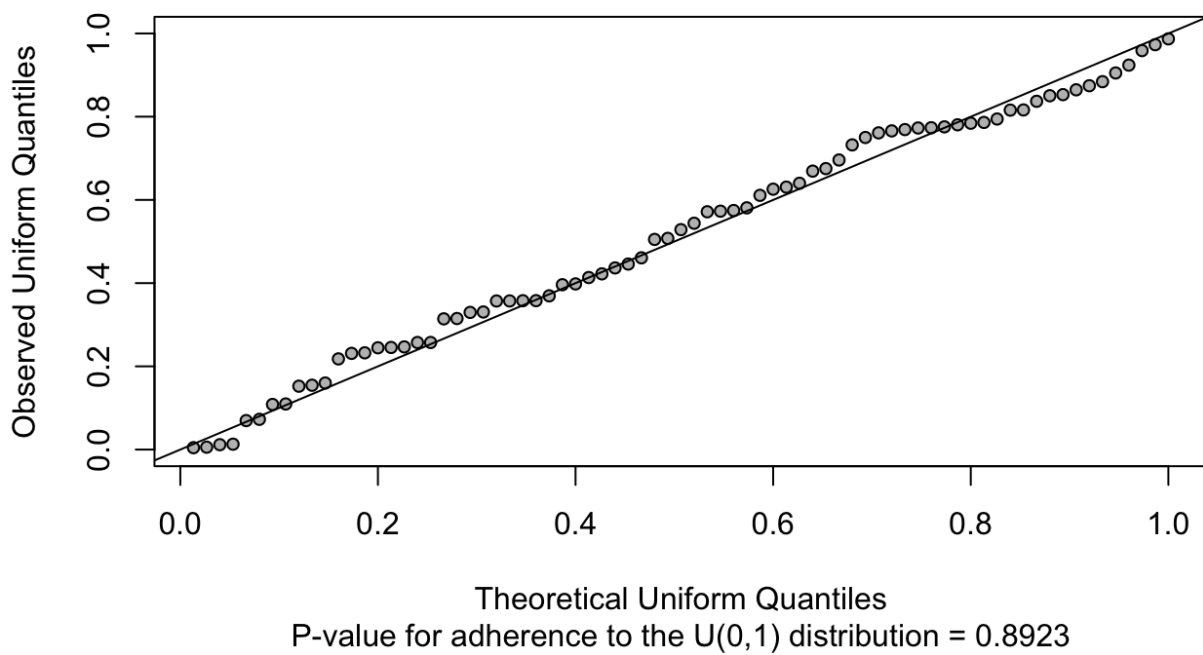


Figure S17. Model control of the Gamma generalized linear mixed model for wind tunnels (WT).

References

- Loubet, B., Cellier, P., Flura, D., & Générumont, S. (1999). An evaluation of the wind-tunnel technique for estimating ammonia volatilization from land: Part 1. Analysis and improvement of accuracy. *Journal of Agricultural Engineering Research*, 72(71), 71–81.